

NATIONAL ADVISORY COMMITTEE
FOR AERONAUTICS

TECHNICAL MEMORANDUMS

Copy 1-2

AUG 23 1924
MAILED

NATIONAL ADVISORY COMMITTEE FOR AERONAUTICS.

Library M.L.

NACA FILE COPY

Loose papers on last
page stamped on back cover

**CASE FILE
COPY**

No. 276

PLEASE RETURN TO

REPORT DISTRIBUTION AND STORAGE SECTION
LANGLEY AERONAUTICAL LABORATORY
NATIONAL ADVISORY COMMITTEE
FOR AERONAUTICS
Langley Field, Virginia

RECENT RESEARCHES IN AIRSHIP CONSTRUCTION - II.

Bending Stresses on an Airship in Flight.

By H. Naatz.

From "Berichte Abhandlungen der Wissenschaftlichen
Gesellschaft für Luftfahrt" (a supplement to "Zeitschrift
für Flugtechnik und Motorluftschiffahrt,") March, 1924.

THIS DOCUMENT IS NOT TO BE REPRODUCED OR TRANSMITTED IN ANY FORM OR BY ANY MEANS, ELECTRONIC OR MECHANICAL, INCLUDING PHOTOCOPYING, RECORDING, OR BY ANY INFORMATION STORAGE AND RETRIEVAL SYSTEM.

NATIONAL ADVISORY COMMITTEE FOR AERONAUTICS
LANGLEY AERONAUTICAL LABORATORY
LANGLEY FIELD, HAMPTON, VIRGINIA

FILE COPY

*17.5
47.3*

To be returned to
file of the Langley
Memorial Aeronautical
Laboratory.

REPORT DIST.
LANGLEY
NATIONAL
SPACE

AS FOLLOWS
NATIONAL ADVISORY COMMITTEE FOR AERONAUTICS
1312 N STREET NW
WASHINGTON 25, D.C.

August, 1924.

26

NATIONAL ADVISORY COMMITTEE FOR AERONAUTICS.

TECHNICAL MEMORANDUM NO. 276.

RECENT RESEARCHES IN AIRSHIP CONSTRUCTION - II.*

Bending Stresses on an Airship in Flight.

By H. Naatz.

In Part I of my lecture I discussed only the stabilization of airships. As the result of my researches, I arrived at the minimum dimensions of control surfaces for rendering an airship manageable under all conditions. I will now discuss the stresses undergone by an airship during flight. I can do this only by comparing individual instances.

Whether an airship is flying straight ahead or in a curve, the mechanical process is always the same, namely, the balancing of the air forces against weights or d'Alembert acceleration forces. Both kinds of forces are held in equilibrium, i.e., their resultants are equal and pass through the same point. The stressing of the airship is due to the fact that these forces are not uniformly distributed. It depends, therefore, on the three questions: 1. How great are the air forces? Then we would also know how great the acceleration forces are; 2. How is the air pressure distributed on the hull? 3. How are the acceleration forces distributed?

We will first consider the air forces and their distribution.

The cases of the inclined airflow are indeed known. We can tell

* From "Berichte und Abhandlungen der Wissenschaftlichen Gesellschaft für Luftfahrt" (a supplement to "Zeitschrift für Flugtechnik und Motorluftschiffahrt"), March, 1924, pp. 55-59.

how great the resulting air force is and where it is located, but not how it originated. Experiments in this connection have been hitherto undertaken only by G. Eiffel (published in 1914), who measured the aerodynamic pressures along several meridians and at different inclinations on the bare models of the "Clement Bayard" and "Fleurus" thus rendering it possible to undertake approximate integrations around several thin disks and determine the resulting lateral pressures. Fig. 17 gives the curves for these pressures. They show that the head of the airship is under positive pressure, but the tail is drawn toward the airflow, which explained the location of the N components in front of the nose of the airship. We may therefore consider these curves, friction being disregarded, as the desired air-pressure curves. Since they have an almost constant appearance on both the "Clement Bayard" and "Fleurus" for all inclinations, we can take, as the basis for our further discussion (since we must resort at times to assumptions), a fundamental curve which can be so shaped that it can be readily plotted from the known C_n and C_m values. In the bottom diagram, this fundamental curve is plotted in conjunction with the curves of the "Fleurus," because the latter comes the nearest to our shapes. Of course, the complete load diagram also includes the horizontal fin and elevator forces, which can, however, be determined accurately enough as trapezoidal and triangular loads with a length corresponding to the control surfaces and with the location of the center of

gravity corresponding to the center of pressure of the control surfaces. We can thus plot the load curve for any inclination, size of horizontal fins and position of the elevator, when the airflow is straight ahead, as, e.g., on an airship in horizontal flight. How is the air pressure affected during evolutions, as, for example, in curving flight and in squalls? In order to answer this question, we must investigate individual cases more thoroughly. In Fig. 18, the airship is flying in a circle and receives an air pressure which is directed inward and whose resultant passes through the center of buoyancy. The airflow is deflected so that the air pressure is greater in the middle than at the nose, and the velocity of flow varies throughout. If, therefore, we can not avail ourselves of experiments with models of a new type (i.e., some kind of revolving apparatus), we must make assumptions. The load diagram is the same here as in rectilinear flow, although in reality, on account of the greater air pressure in the middle, it is less pronounced and hence more uniform. Moreover, we are not concerned about the direction of the flow with reference to the center of buoyancy and, likewise, regarding the speed of the airship, but we assume the maximum air force N with rectilinear flow and a given thrust. Thus, e.g., we find, according to the rules governing the calculation of the longitudinal stability, that the shape 1505 gives nearly the maximum value for the N component, if it is to pass through the center of buoyancy, at an inclination $\alpha = 13.2^\circ$

and, in fact, is

$$N = 0.1108 V^{2/3} q = \frac{11.08}{100} V^{2/3} q,$$

in which V = the air displacement, q , the dynamic pressure due to the speed of the airship in horizontal flight and $\alpha = 0^\circ$.

Here the coefficient,

$$C_n = 11.08,$$

is composed of the coefficient of the bare hull and the coefficient of the horizontal fins reduced to $V^{2/3}$. The fins have the size $\frac{F}{V^{2/3}} = 0.2375$ and are placed with their trailing edges 0.1L from the stern. We adopt this C_n value, as also its load diagram, as the basis of circular flight, under the assumption that it can not be greater in circular flight. We will later compare the maximum bending moments with actual results. If there is approximate agreement, it will show that our assumptions have not been unwarranted. After the air-pressure diagram has once been determined, the plotting of the load by means of acceleration forces is then a simple matter. Here, in circular flight, the weights are distributed likewise. They are, however, distributed approximately as the lifts in individual places. Hence the load curve can be plotted proportionally to the load curve of the airship. We will take this matter up again, after considering other cases of flow.

If an airship is flying straight ahead and, at the same time is turning about its center of gravity, there arises the flow picture shown in Fig. 19. From the similarity of the triangles

OBS and BCD, it may be readily deduced that

$$\rho_s = \frac{v}{\omega} \quad \text{and} \quad v_1 = v \frac{\rho}{\rho_s}$$

in which ω is the angular velocity of the airship. The flow is therefore deflected concentrically about the center, as if the airship were flying in a circle. The case of simultaneous flight and rotation is actually very rare, since the rotation is usually caused only by a resultant lateral force, so that the usual case (e.g., in oscillations of the airship) is a combined rotation and circular flight. Fig. 20 gives the flow diagram for the latter case. From the similarity of the triangle ECD to O'BS and of BED to BO'O it may be likewise deduced that

$$\rho_2 = \frac{v}{\omega + \frac{v}{\rho_1}} \quad \text{and} \quad v_2 = v \frac{\rho''}{\rho_2}$$

i.e., the airflow in circular flight will be deflected still more, if the airship turns at the angular speed ω with respect to ρ_1 . In circular flight, however, if the airship retains its inclination to ρ_1 , it makes, with respect to a fixed line in space, the turn

$$\omega_1 = \frac{v}{\rho_1}$$

Hence, we may write

$$\rho_2 = \frac{v}{\omega + \frac{v}{\rho_1}} = \frac{v}{\omega + \omega_1} = \frac{v}{\omega_0}$$

From this it follows that the deflection of the flow is directed only according to the angular velocity ω_0 of the airship with respect to the horizontal plane or with respect to the north

and south plane. This holds good both for calm and moving air, but not for gusts, since a gust is a local disturbance in either quiet or uniformly moving air and is contrary to the previous assumption of homogeneity. If a horizontal section is made through a gust, there is obtained the diagram (Fig. 21) of velocities with respect to the surrounding air regarded as at rest. If these velocities are combined with the speed of the airship, the lower diagram is obtained, which can represent the flow for an airship flying in a gust. It resembles the curved flow with which we are already acquainted, excepting that the curve is not everywhere concentric and the velocities do not increase regularly outward.

Nevertheless, it may be said that the air pressure does not differ materially from that during the turning of the airship, more especially as the phenomenon does not take place without a turning of the airship. From an inspection of all the flow diagrams, we can repeat what we said in connection with circular flight, namely, that, in all cases, the load diagram and likewise the corresponding maximum C_n values can be taken from the direct flow. We need only to compute the following cases, in order to embrace all other cases.

1. Maximum air force in the center of buoyancy of the airship, acceleration forces distributed according to the lifts (circular flight).

2. Maximum air force in the oblique position with extreme

rudder deflection (circular flight and turning).

3. Maximum rudder force.
4. Airship heavy in the middle and supported aerodynamically.

In Fig. 22, the first case for the shape 1505 is computed.

The maximum value for the N component of the air force is

$$N = 0.1108 V^{2/3} q$$

in which q = the dynamic pressure for $\alpha = 0^\circ$ and $\beta = 0^\circ$. The maximum bending moment is reached at $0.55L$ and is

$$M_1 = 0.008 V^{2/3} q L.$$

This form of the expression can be applied to any other airship, if the volumetric efficiency is approximately the same, namely, $\delta = 0.345$. In determining the maximum bending stress, however, this is not the decisive moment, but another whose ratio to the moment of resistance reaches the highest value at the time. The moment of resistance or drag of the airship is compared in a practical manner with that of the thin-walled tube and written as follows:

$$W = \pi r^2 d,$$

in which r = radius of cross-section and d = thickness of wall. If the cross-section is a circle and the material of uniform thickness, instead of dividing the moments found by the temporary W values, we can so compute the moment curves that they will apply only to the maximum cross-section. In this case, if r_0 = the radius of the principal cross-section, the reduction factor would

that the weights are distributed correspondingly to the lifts. Lastly, we consider the phenomenon as a lateral motion of the airship, in connection with which there are no further axial forces to take into account. In vertical motions (e.g., the moment of stability) trim and other axial forces would have to be considered, which would go beyond the scope of our general discussion. Most airships, on account of the walkways, etc., resist vertical bending more than lateral bending, so that we can disregard the distinction.

The acceleration force of a disk of the thickness dx is

$$dQ = p \frac{\gamma}{g} F dx + \epsilon (0.5582 L - x) \frac{\gamma}{g} F dx,$$

in which the quantity $0.55026 L =$ the distance of the center of buoyancy from the trailing edge. From this expression we can, however, obtain

$$dQ = N \left(\frac{F_0}{V^{2/3}} \right) \left(\frac{L}{V^{2/3}} \right) \left(\frac{F}{F_0} \right) \left[1 + \left(0.5582 - \frac{x}{L} \right) \frac{e}{L} \frac{L^2}{K^2} \right] d \left(\frac{x}{L} \right)$$

or

$$dQ = N \frac{1}{\delta} \left(\frac{F}{F_0} \right) \left[1 + \left(0.5582 - \frac{x}{L} \right) \frac{e}{L} 21.2 \right] d \left(\frac{x}{L} \right)$$

in which $F =$ area of cross-section at the point x ,

$F_0 =$ area of largest cross-section,

$L^2/K^2 = 21.2$ by computation and remains the same for all distance ratios, when δ is moderate.

Fig. 23 gives the corresponding curves and integrations.

Here

$$N = 0.117 V^{2/3} q$$

$$\left(\frac{F}{V^{2/3}} = 0.2375, \frac{Fr}{F} = 0.15 \right)$$

is found by computation. The maximum reduced bending moment is

$$M_3 = 0.0103 V^{2/3} q L$$

or

$$M_3 = 0.088 N L$$

Still larger bending moments are obtained in case 3 by working the rudder. In Fig. 24, for the sake of simplicity, the values $N = 1$ and $e/L = 0.438$ are adopted. A maximum value is thus obtained, which, however, already lies in the field of the fins, of

$$M_3 = 0.223 N L,$$

or more commonly calculated, when various locations of the force N are adopted, together with the moments for the position $0.35L$ where the leading edge of the fin lies

$$M_1 = \left(0.828 \frac{e}{L} - 0.232 \right) N L$$

or

$$M_3 = M_1 1.57 = \left(1.3 \frac{e}{L} - 0.364 \right) N L,$$

or, when x = distance of center of rudder force from rear end of airship

$$M_3 = \left(0.362 - 1.3 \frac{x}{L} \right) N L.$$

$\frac{x}{L} = 0.12$ may be adopted as an extreme case and then

$$M_3 = 0.206 N L$$

This force N is computed, with the aid of the diagram (Fig. 9, Part I) on the basis of the following data:

$$\frac{F_r}{F} = 0.15, \quad \frac{F}{V^{2/3}} = 0.2375,$$

with trailing edge of rudder at $0.1L$ and $\beta = 20^\circ$, to

$$N = 0.068 V^{2/3} q \left(\frac{2.18}{2.93} \right)^{2/3} = 0.0558 V^{2/3} q,$$

so that we obtain for the bending moment a maximum value of

$$M_3 = 0.0115 V^{2/3} q L$$

This value remains approximately the same for larger rudders, because the resulting center of pressure on the rudder then moves nearer the center of buoyancy.

Regarding the bending from the acceleration forces, there remains only case 4, namely, with the airship heavy or light in the middle. Ordinarily, this case would introduce nothing especially new, since it can be compared with case 1. Heaviness or lightness at the ends likewise causes no special stresses, since load and support are related in their nature. On the contrary, we may term an airship heavy or light in the middle (e.g., the emptying of one or two cells as a heavy case), since load and support here differ greatly from each other, as shown by Figs. 25-26. In fact, the greatest stresses are thus caused, e.g., according to Fig. 26,

$$M_3 = 0.0185 V^{2/3} q L,$$

whereby

$$N = 0.117 V^{2/3} q.$$

If care is taken, however, that the increase or decrease in weight of the airship, if really limited to a short space, does not exceed a certain amount (say, the lift of one to two cells), it can only be determined for each case, as to whether the value found for M_3 is attained in practice. The emptying of cells is a damage, which can always be diminished by releasing or transferring ballast.

Aside from this exceptional case, which, moreover, affects only the vertical bending, the deflection of the rudder exerts the greatest stresses on the airship. The here possible value

$$M_3 = 0.0115 V^{2/3} q L$$

must now be verified in practice. In this respect nonrigid airships are the best, because the rigidity of the hull is the result of the inflation and the functioning pressure and is only increased until deformations disappear or cause no further trouble. Such was PL27, a type lying in the field of our discussion, which made about 24 m (787 ft.) per second and which, during its life of more than two years, mastered the worst squalls with only 20-25 kg/m² (4.1-5.1 lb./sq.ft.). The deformations in the vertical plane were not noticeable and the maximum bending in the horizontal plane did not exceed 0.75%. If we should assume, however, that the rigidity of the airship would be overcome at an operating pressure of 20 kg/m² (4.1 lb./sq.ft.), we would come to the con-

and an air displacement of 32000 m³ (1,130,000 cu.ft.), hence at $V^{2/3} = 1008 \text{ m}^2$ (10850 sq.ft.). We can now write

$$M = x V^{2/3} q L$$

or

$$56850 = x 1008 \times 36 \times 157 = x 570000,$$

so that

$$x \approx 0.01,$$

while we have previously found $x = 0.0115$, i.e., our computations on the basis of aerodynamical experiments were not unwarranted and the maximum values are hardly attained in practice. We may consider it a rule that every airship must be able to withstand a bending moment of $M = 0.01 V^{2/3} q L$. In addition to bending, shear and torsion also play a certain role. Since, however, this question is closely connected with the question of the strength of the individual parts affected by the forces (e.g., the fins and rudders), it belongs to the realm of construction and does not need to be expressed here.

On the other hand, the maximum fin and rudder load is worth knowing. We may here abide by the previously calculated maximum values of C_n , by saying (with the same right as we deduced the maximum bending moments from the maximum air forces with consideration of the decrease in speed) that we can deduce the surface loading from the same forces. The following table gives the C_n values from the previous calculations.

α	β	A Fin C _n with respect to area	B Rudder		$\left(\frac{v}{v_0}\right)^2$	Reduced values		Total
			C _n with reference to area	C _n with reference to $3 F_r$		A	B	
0°	20°	--	28.6	63.5	0.82	--	52.0	52.0
13.2°	0°	89.0	--	--	0.392	34.8	--	34.8
13.2°	20°	89.0	28.6	63.5	0.333	29.6	21.1	50.7
15°	20°	109.0	28.6	63.5	0.284	31.0	18.0	49.0

The rudder pressure is here taken with respect to $3 F_r$, since, as we have previously seen, the center of pressure, in great deflections, lies at about 0.5 the depth of the rudder from the rudder axis. If we further consider that only 73% of the pressures calculated are exerted on the control surfaces, we arrive at fin pressures with zero rudder deflection: $p = 0.254 q$ and maximum pressure on the rudder and its vicinity: $p = 0.38 q$. For $v = 35$ m (115 ft.) per second, we would thus obtain 19.5 and 29 kg/m² (4 and 5.9 lb./sq.ft.).

In conclusion, we will add a brief discussion on increasing the size of airships. We have seen that the maximum bending moment may be expressed by the formula

$$M = 0.01 V^{2/3} q L$$

and that we can offset this moment with an internal pressure, which may be found as follows

$$p_m = \frac{M}{\pi r^3} \times \frac{3}{3}$$

in which x = the coefficient for the moment of inertia of the cross-section with respect to its axis. Or

$$p_m = \frac{0.01 \sqrt{2/3} L}{x \frac{\pi r^3}{3}} q = \frac{0.03}{x} \frac{(2n)^{5/3} \delta^{2/3}}{\pi^{2/3}} q,$$

$= \pi^{1/3}$

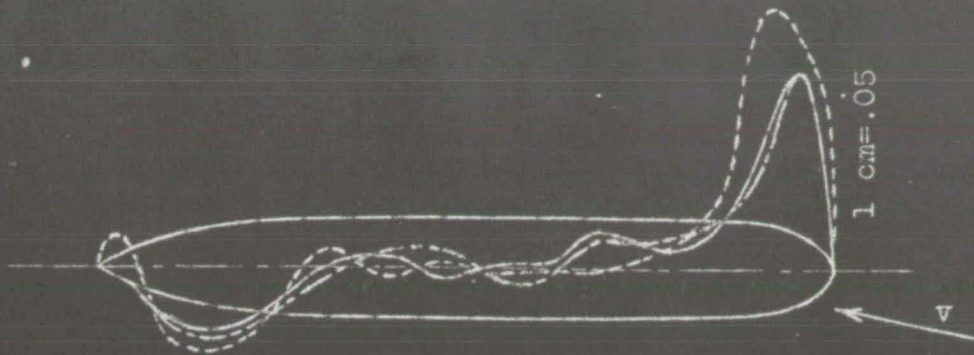
in which $n = L/2r$, so that also

$$p_m = 0.0435 \frac{n^{5/3} \delta^{2/3}}{x} q.$$

$S = \frac{V}{\pi L R}$
per TM 275
fig 5

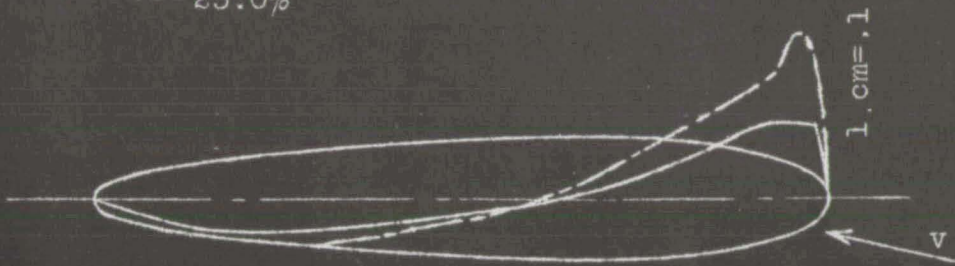
If we consider the mean inside pressure as the counter-pressure against the external forces, on the basis of this formula we can say:

1. The counter-pressure varies directly as the dynamic pressure.
2. It increases considerably with the elongation ratio of an airship.
3. It remains the same for large and small airships, from which it follows that:
 - a) Long airships should be avoided, since they have neither aerodynamic nor structural nor navigational advantages;
 - b) There appears to be no objection to increasing the size of airships. For nonrigid airships, this leads indeed to smaller pressures while flying, since p_m = the operating pressure plus the gas pressure at the equator, which increases with the size of the airship.

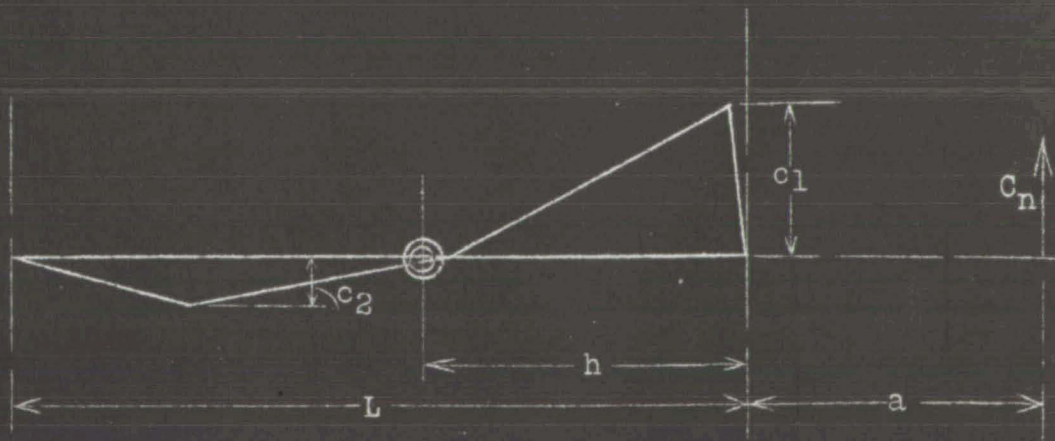


Clement - Bayard

- 7.5%
- - - 15.0%
- - - 25.0%



Fleurus



$$c_1 = 8.62 \frac{C_n}{100} \left(\frac{a}{L} + 0.72 \right) \frac{1}{L}$$

$$c_2 = 5.75 \frac{C_n}{100} \left(\frac{a}{L} + 0.14 \right) \frac{1}{L}$$

$$\frac{a}{L} = \frac{C_m}{C_n} \frac{V^{1/3}}{L} - \frac{h}{L}$$

Fig.17 Distribution of air load.

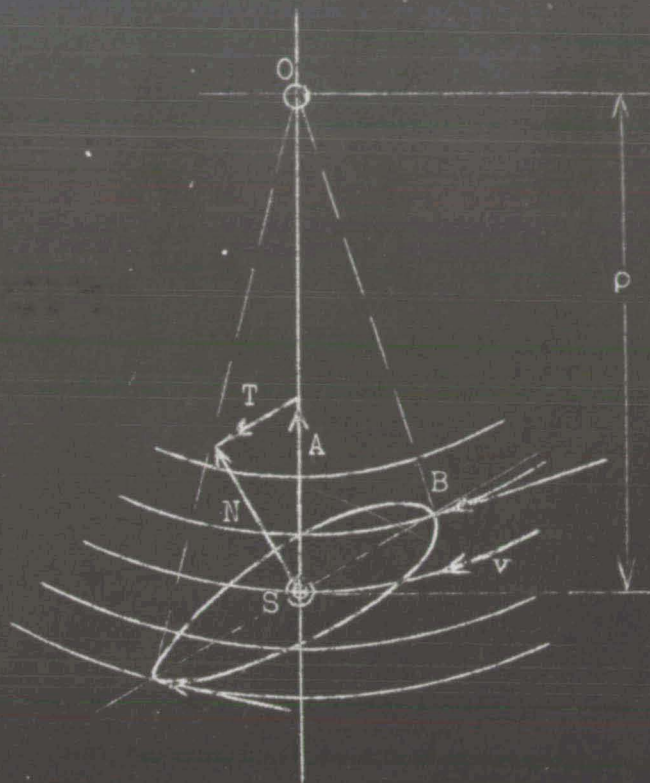


Fig. 18 Circular flight.

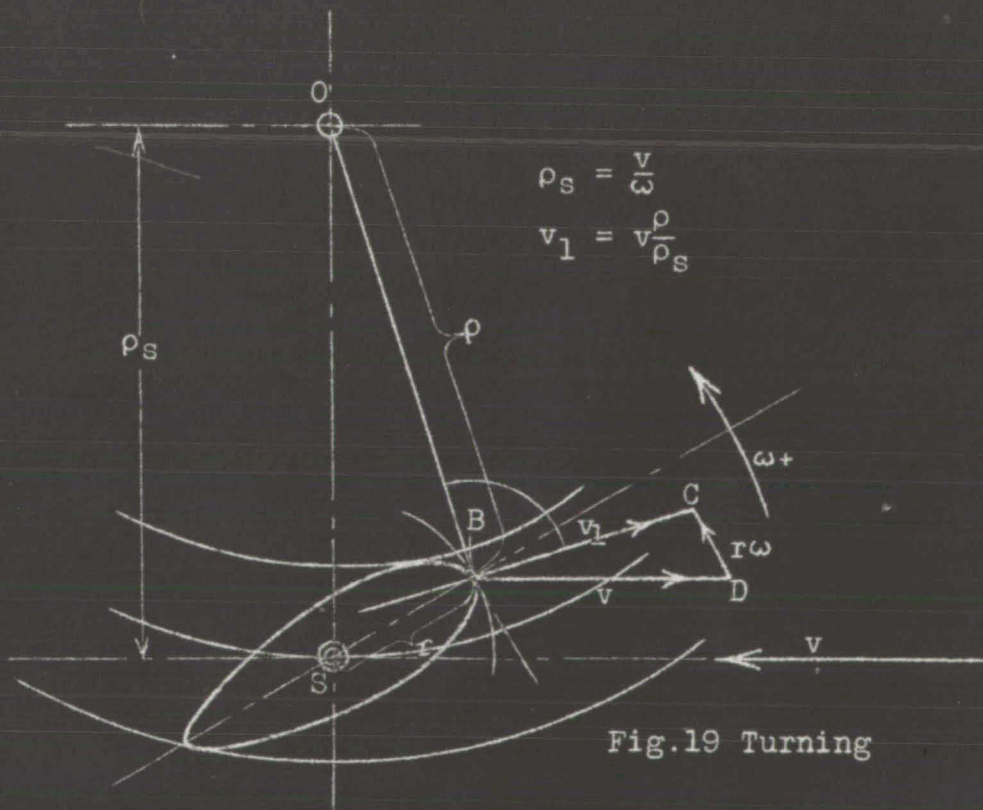


Fig. 19 Turning

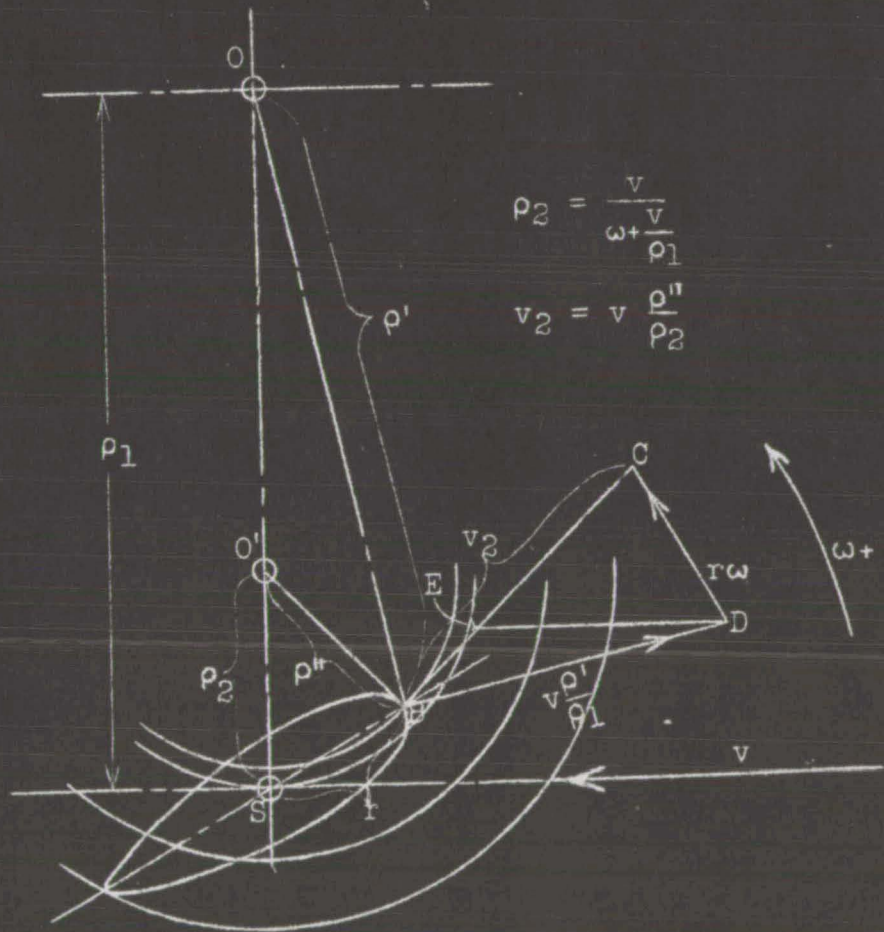


Fig. 20 Circular flight and turning.

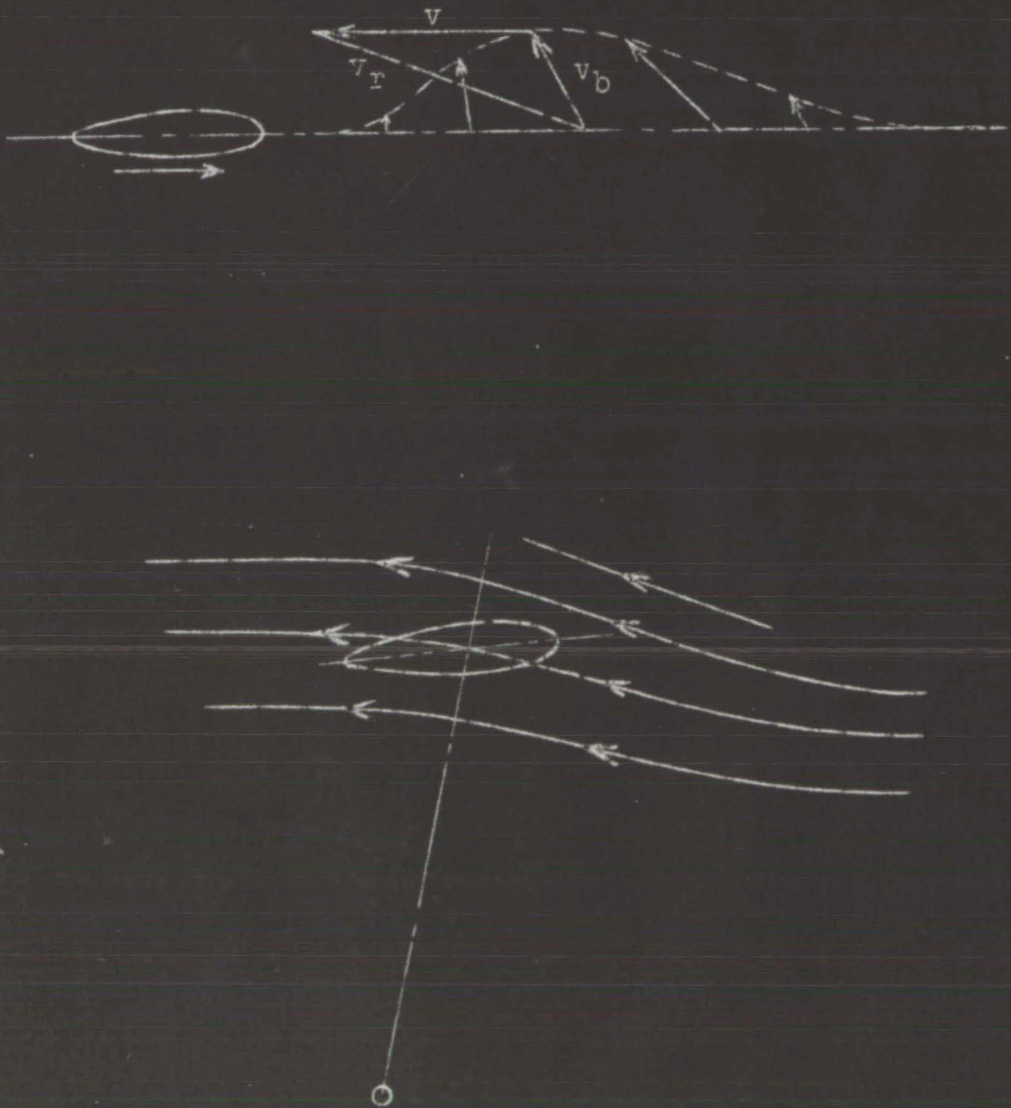


Fig. 21 Flow in a gust.

Airship form 1505,
 $\alpha = 13.2^\circ$, $\beta = 0^\circ$

$F/V^{2/3} = .2375$

$F_T/F = 0.15$

Resultant in center of buoyancy \odot

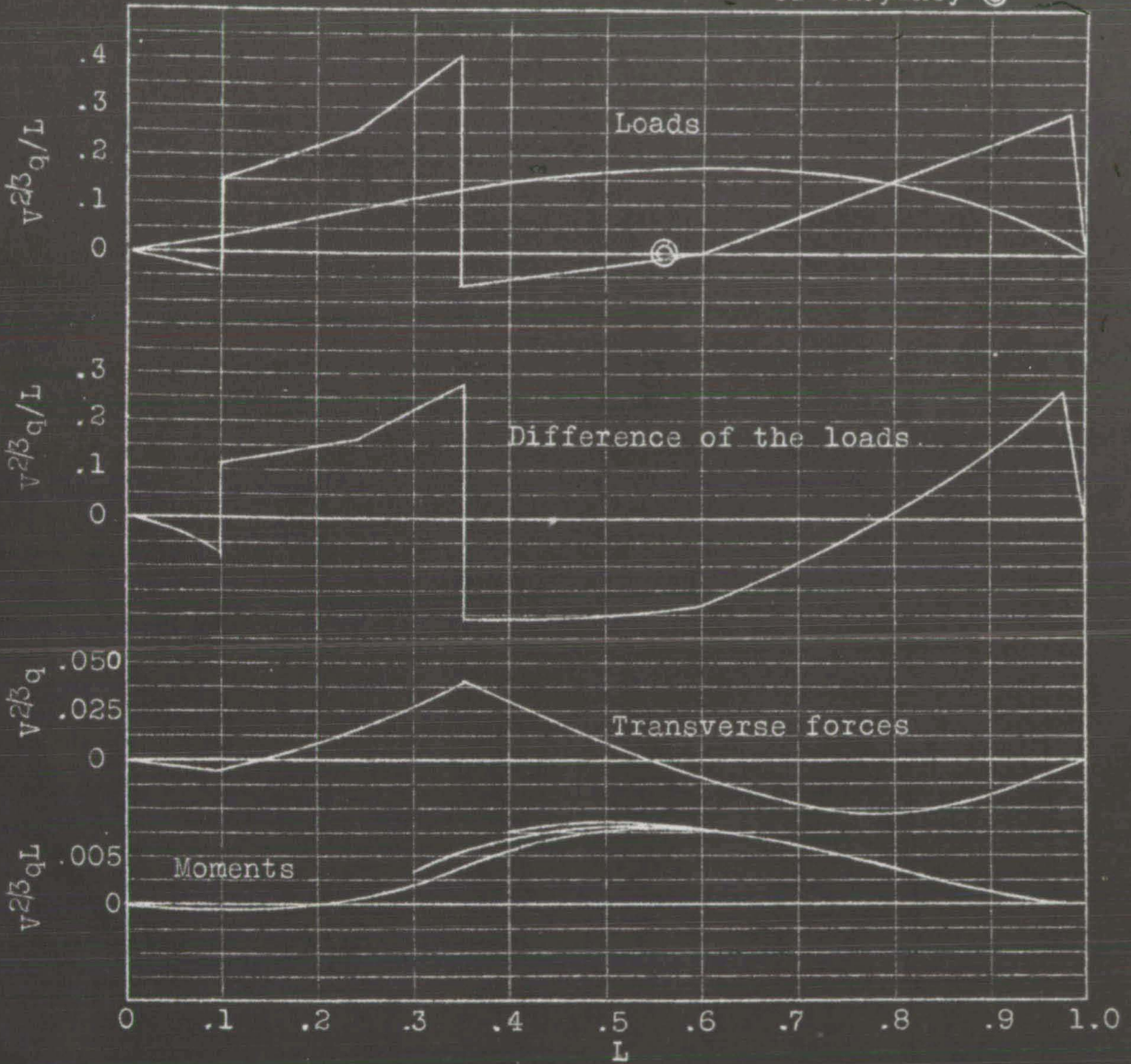


Fig.22 Forces due to air and gravity.

Airship form 1505.

$\alpha = 13.2$, $\beta = 20^\circ$

$F/v^2\beta = .2375$

$F_r/F = 0.15$

Resultant in center of buoyancy \odot

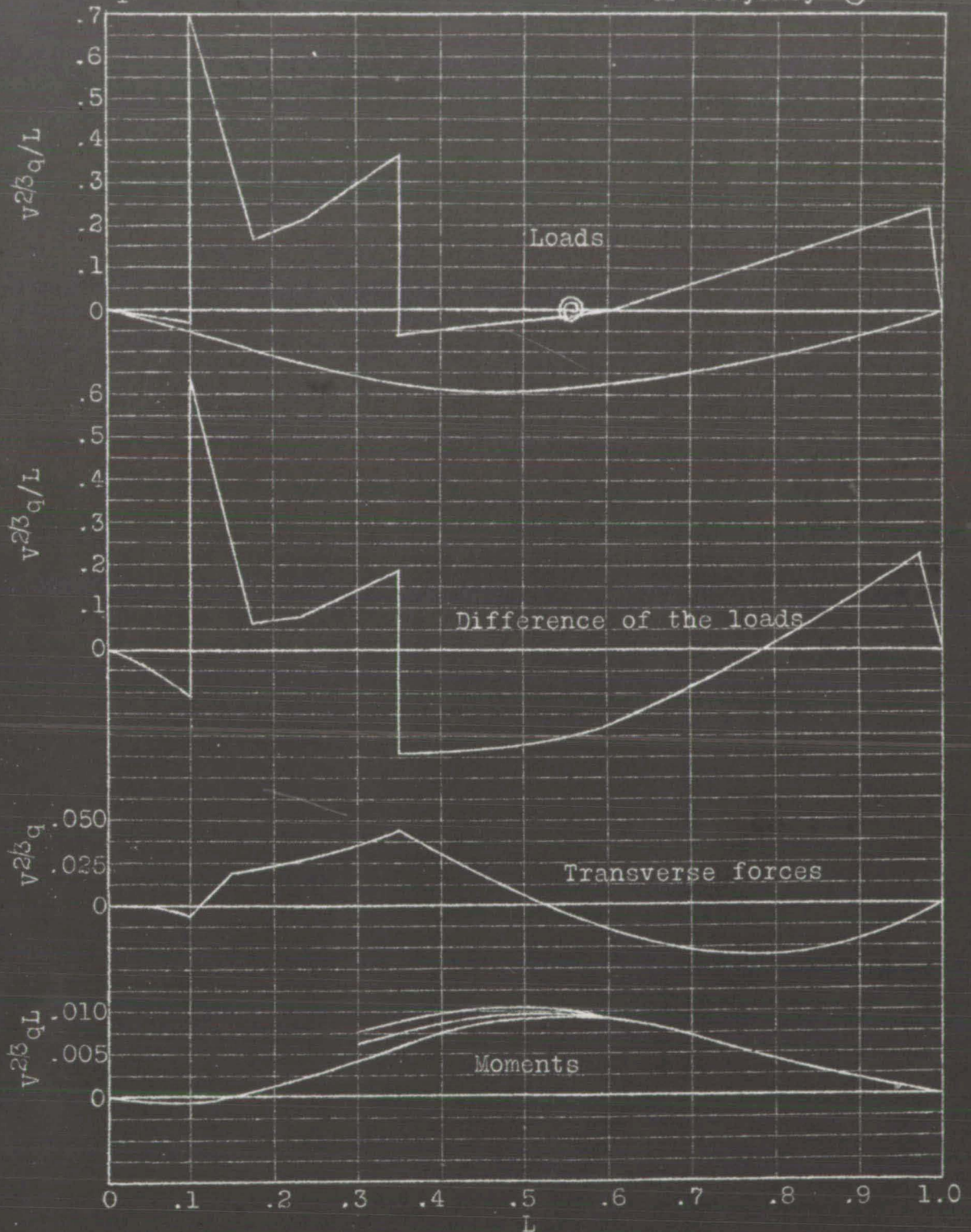


Fig.23 Forces due to air and gravity.

$\alpha = 0^\circ$

Form 1505

$\beta = 20^\circ$

Resultant in center of buoyancy \odot

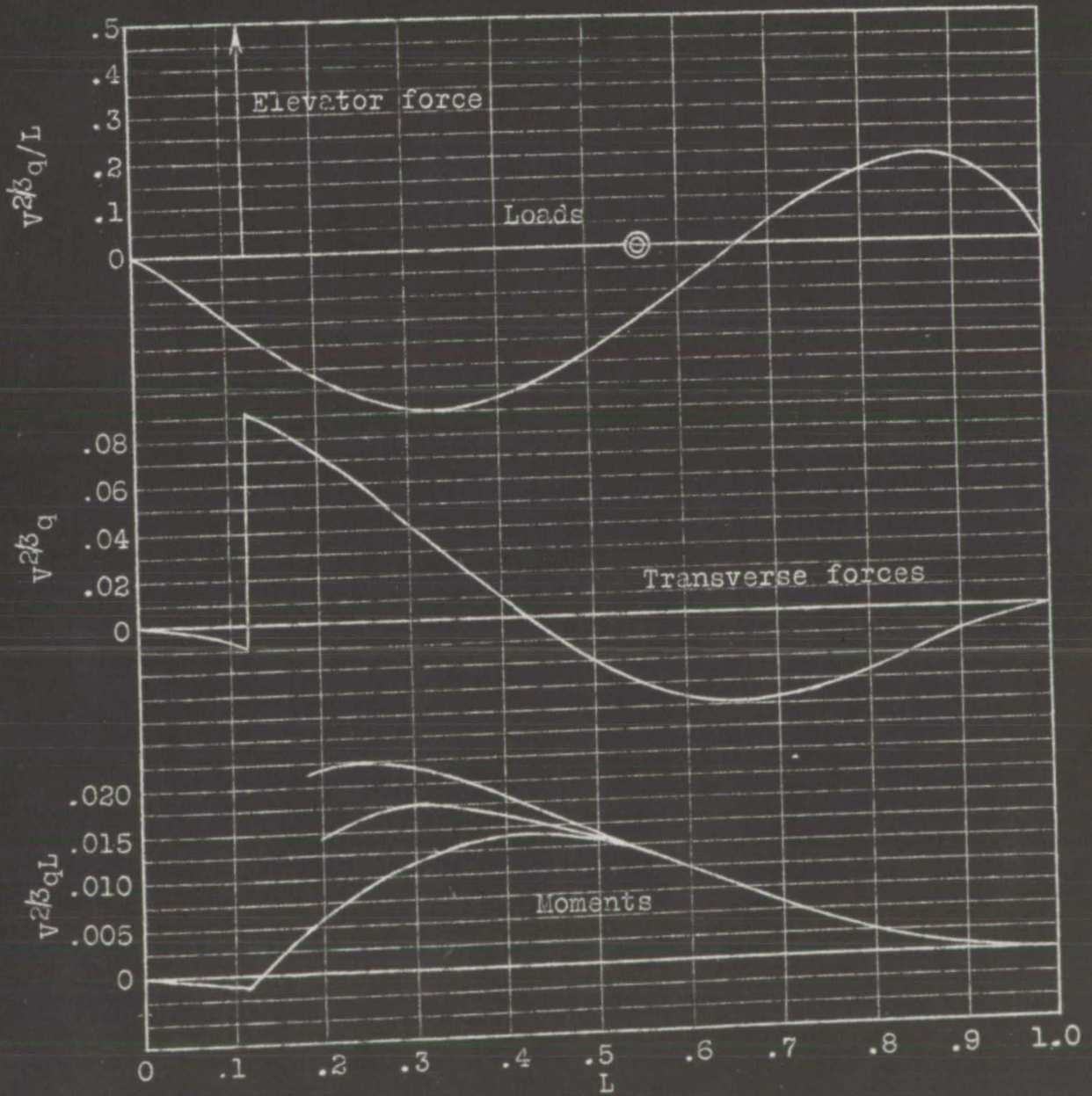


Fig. 24 Elevator and gravity forces.

24

Airship form 1505
 $F/V^{2/3} = .2375$
 $\alpha = 13.2$ $\beta = 0^\circ$
 $F_r/F = 0.15$

Resultant in center of buoyancy \odot

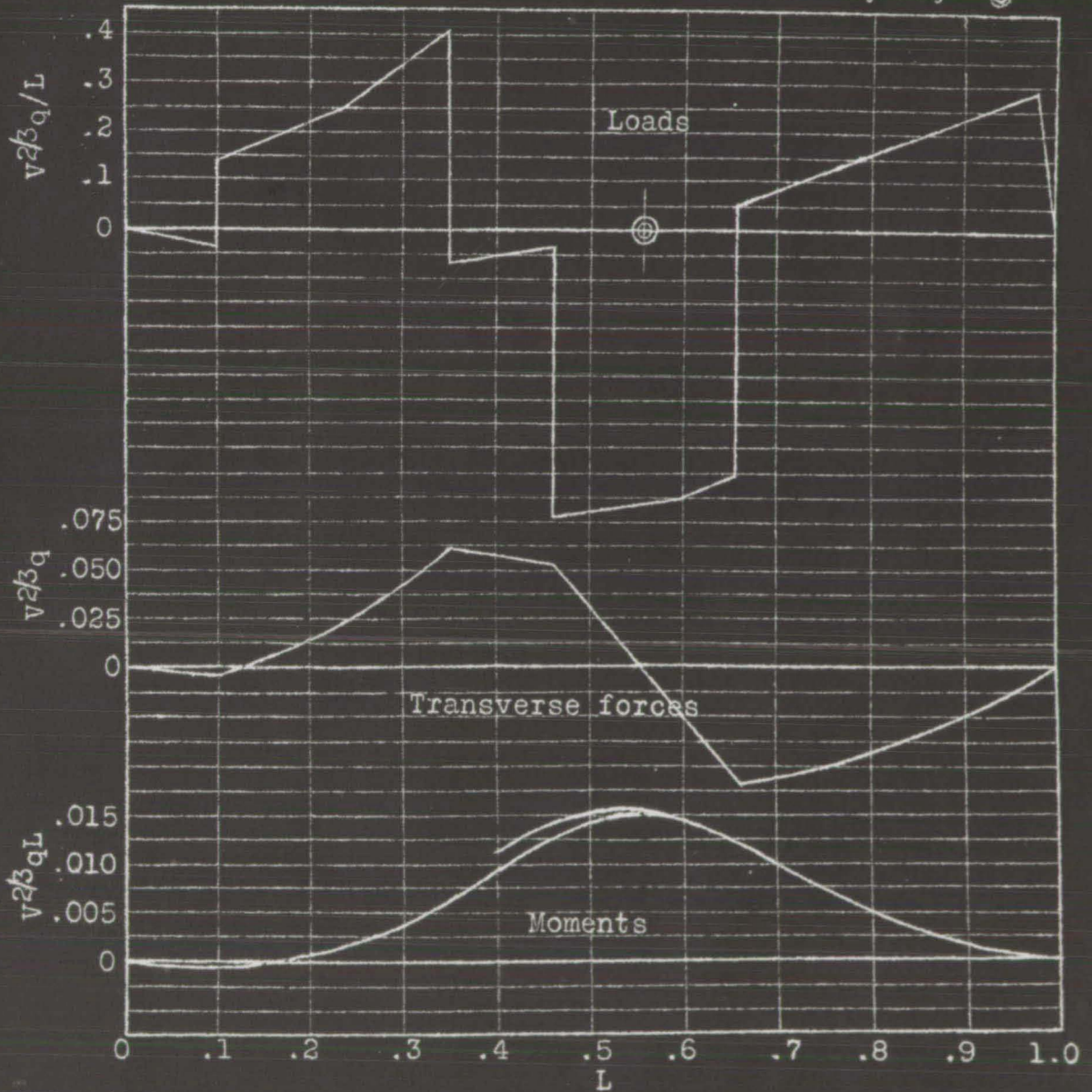


Fig.25 Air forces and separate loads.

$F/v^2\beta = .2375$

Airship form 1505

$\alpha = 13.2 \quad \beta = 20^\circ$

$F_T/F = 0.15$

Resultant in center of buoyancy \odot

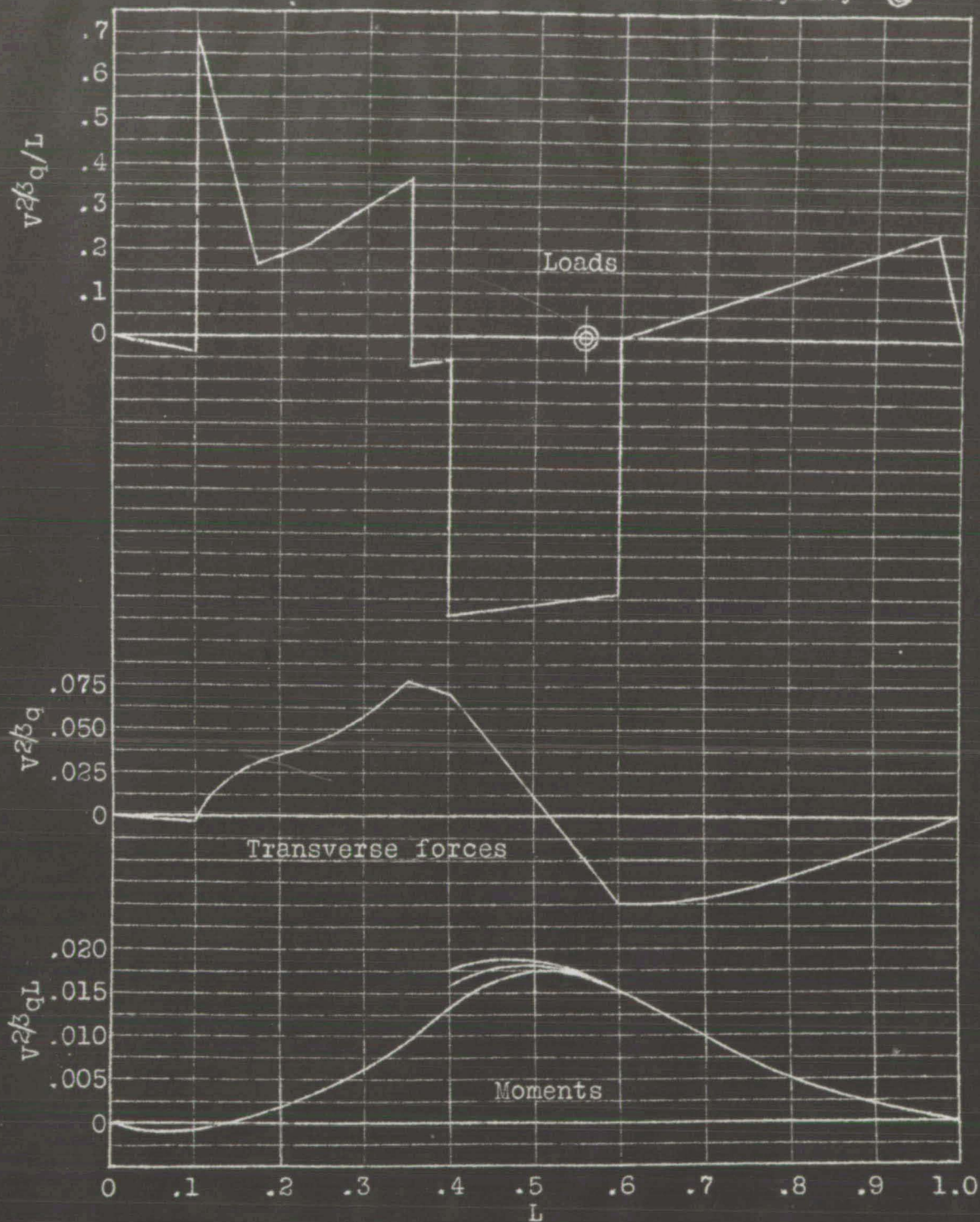


Fig.26 Air forces and separate loads.